Annals of Anatomy 246 (2023) 152044

Contents lists available at ScienceDirect

Annals of Anatomy

journal homepage: www.elsevier.com/locate/aanat

Research article

# Somatostatin: From a supporting actor to the protagonist to explain the long-term effect of sleeve gastrectomy on glucose metabolism

Gonzalo-Martín Pérez-Arana [c,d,*], Alfredo Díaz-Gómez [f], José Bancalero-de los Reyes [a], Alonso Camacho-Ramírez [b,d], Antonio Ribelles-García [c], David Almorza-Gomar [d,e], Manuel Gracia-Romero [c], Isabel Mateo-Gavira [g], José-Arturo Prada-Oliveira [c,d,*]

[a] Complejo Hospitalario de Badajoz, Servicio Extremeño de Salud, Spain
[b] Surgery Unit, Puerta del Mar University Hospital, University of Cadiz, Spain
[c] Department of Human Anatomy and Embryology, University of Cadiz, Spain
[d] Institute for Biomedical Science Research and Innovation (INIBICA), University of Cadiz, Spain
[e] Operative Statistic and Research Department, University of Cádiz, Spain
[f] San Carlos Hospital, Andalusian Health System, Spain
[g] Endocrine and Nutrition Service, Puerta del Mar University Hospital, University of Cadiz, Spain

ARTICLE INFO

*Article history:*
Received 7 October 2022
Received in revised form 9 December 2022
Accepted 11 December 2022
Available online 28 December 2022

*Keywords:*
Pancreas
Sleeve gastrectomy
Type 2 diabetes mellitus
Bariatric surgeries
Somatostatin

ABSTRACT

*Background:* Bariatric/metabolic surgery has become the most effective treatment against type 2 Diabetes mellitus (T2DM). The role of many gastrointestinal hormones in T2DM has been proposed, but the pathophysiological models described vary greatly depending on the anatomical rearrangements after surgery. We focus on somatostatin as a common factor in two of the most commonly performed surgical procedures in a healthy rodent model. We performed sleeve gastrectomy (SG) and Roux-en-Y gastric bypass (RYGB) and also an experimental surgery without gastric involvement (intestinal resection of 50 % jejunum-ileum portion –IR50 %). Methods: We used five groups of Wistar rats: fasting control, sham-operated, SG-operated, RYGB-operated and IR50-operated. We analysed several parameters 4 and 23 weeks after surgery: plasma SST-14/28 fractions, plasma glucose, insulin release and SST-producing cell expression in the duodenum and pancreatic islets. Results: Numerous SST-producing cells in the duodenum but a low number in the pancreas and a long-term loss of glucose tolerance were observed in SG and RYGB animals. Additionally, a high plasma SST-28 fraction was found in animals after SG but not after RYGB. Finally, IR50 animals showed no differences versus controls. Conclusions**:** In our SG model the amplitude of insulin response after metabolic surgeries, is mediated by SST-28 plasma levels derived from the proportional compensatory effect of gastric SST-producing tissue ablation. In addition, a strong compensatory response to the surgical loss of gastric SST-producing cells, leads to long-term loss of insulin production after SG but not in the others.


## 1. Background

Currently, bariatric/metabolic surgeries are a powerful tool to treat type 2 diabetes mellitus (T2DM). This approach is even better than most pharmacological management strategies (Schauer et al., 2017). Among these surgeries, two of the most effective and widespread bariatric/metabolic surgeries are Roux-en-Y gastric bypass (RYGB) and sleeve gastrectomy (SG) (Alsumali et al., 2018). Significant postsurgical anatomic rearrangements differentiate them. RYGB implies stomach division into a small upper pouch and a larger lower pouch. The small intestine is divided and rearranged into a Y-configuration and the connection of the "Roux limb" to the small upper stomach pouch (Mun et al., 2001). Alternatively, SG removes a part of the stomach along the major curvature involving the antrum and fundus without any intervention on the small intestine (Benaiges et al., 2015). Both methods lead to quick improvement in T2DM even after weight loss (Schauer et al., 2017). A handful of theories have been devised to explain this effect. Many authors have

*Abbreviations:* EDTA, Etilen Diamiano Tetracetic acid; FC, Fasting control; GLP-1, Glucagon Like Peptide −1; PYY, Peptide Tyrosine-Tyrosine; IR50, Resection technique of 50 % of the intestine; OGTT, Oral glucose tolerance test; RYGB, Roux-en-Y gastric bypass; SG, Sleeve gastrectomy; SST, Somatostatin; T2DM, Diabetes Mellitus Type 2

* Corresponding authors at: Department of Human Anatomy and Embryology, University of Cadiz, Spain.
*E-mail addresses:* gonzalo.perez@uca.es (G.-M. Pérez-Arana), arturo.prada@uca.es (J.-A. Prada-Oliveira).

https://doi.org/10.1016/j.aanat.2022.152044

proposed anatomical rearrangements after RYGB as responsible for the high incretin released due to the early arrival of food to the ileum and jejunum. In this sense, high glucagon-like peptide-1 (GLP-1) and/or peptide tyrosine-tyrosine (PYY) postprandial plasma levels have been analysed in patients and animal models (Camacho-Ramírez et al., 2020a, 2020b; Guida et al., 2018; Shah et al., 2019). Other studies have tried to explain T2DM improvement based on the beneficial effect of these incretins on the beta-cell population and its capacity for insulin secretion (Guida et al., 2019; Nauck, 2016). Nevertheless, the participation of some of these is doubtful, as demonstrated by (Mokadem et al., 2013), who achieved glucose level restoration in RYGB-operated GLP-1-deficient diabetic mice.

SG is another bariatric/metabolic surgery in which an important part of the stomach is eliminated, also removing the ghrelin-producing cell population and leading to a drop in circulating ghrelin. Many other studies have suggested the improvement of diabetes based on SG (Santiago-Fernández et al., 2017). However, the role of ghrelin after SG is not clear. A recent study proposed residual epsilon ghrelin-producing cell expansion in the pancreas as a response to antrum and fundus ghrelin-producing cell loss after SG with sustained plasma ghrelin levels in rats (Camacho-Ramírez et al., 2020a, 2020b).

In addition, both surgical outcomes display a high percentage of T2DM relapse five years after surgery: 33.1 % in RYGB and 41.6 % in SG (McTigue et al., 2020). Recent articles propose a long-term beta-cell population loss in healthy Wistar rats after SG and RYGB with an elevation in postprandial glucose levels (Bancalero-de los Reyes et al., 2021; Pérez-Arana et al., 2022a, 2022b).

There is a loss of somatostatin-secreting cells in the stomach in both surgeries. Somatostatin (SST) is an inhibitory hormone with two biologically active isoforms, SST-14 and SST-28. The latter isoform is predominant in the blood circulation after a meal, but both are mostly secreted by the stomach. Additionally, SST-14 delta cell secretion has been described in pancreatic islets (Francis et al., 1990). Delta cells have paracrine inhibitory activity on beta cell populations (Benso et al., 2003). But also SST-14, it is a paracrine inhibitor of glucagon secretion by alpha-cells within pancreatic islets (Xu et al., 2020).

In this sense, a recent study reported duodenal SST-producing cell expansion as a compensatory response to stomach SST-secreting tissue ablation after SG, triggering a loss of the delta cell population and paracrine SST-14 activity in the islet, leading to long-term postprandial plasma insulin depletion due to beta cell population exhaustion in rats (Perez et al., 2022a).

Taken together, these data raise the possibility that may be a different common element behind the improvement and relapse of diabetes after RYGB and SG surgery.

In the present study, we investigated the role of SST on the pathophysiological basis of glucose metabolism improvement after RYGB compared with the proposed model for the SG using healthy Wistar rats. To complete the study, we introduce IR50, a malabsorptive experimental metabolic surgery, which involves 50 % small gut resection, including resection of the length of the jejunum and ileum, without anatomic rearrangement of the stomach.

## 2. Material and methods

All animal procedures were previously studied and approved by The Committee for ethical Use and Care of experimental animals at Cadiz University. Thirty Wistar male rats weighing 200–220 g at an age of 10–11 weeks were provided and kept at the Experimentation and Animal Production Service of University of Cadiz (SEPA).

### 2.1. Experimental protocol

The rats were randomly divided into five groups: n = 6 fasting control (FG) rats; n = 6 sham-operated (Sham) rats; n = 6 sleeve gastrectomy-operated (SG) rats; n = 6 Roux-en-Y gastric bypass-operated (RYGB) rats; and n = 6 50 % small gut resection-operated (IR50) rats. All animals were sacrificed twenty-four weeks after surgery.

The FG group animals (n = 6) underwent the same perioperative fasting periods, related to the surgical protocol. All animals completed 12 h presurgical and 12 h postsurgical fasting periods. An intake readaptation period followed surgery to normalize fasting and a weight measurement every three days from surgery to the fifth week of survival were performed.

### 2.2. Surgical procedures

The surgical procedures were always performed in anaesthetized animals using continuous infusion of Isofluorane 2–4 % V/V (Abbott Columbus, OH, USA).

The sham technique (Sham) (n = 6) reproduced the surgical aggression over the stomach and gut, but the Sham maintained its integrity. Sham was performed by a laparotomy of 5 cm in the upper third of the abdomen and an incision of approximately 3 cm in the middle area of the abdomen, sectioning the gastrosplenic ligament and exposing the stomach. The jejunum was transected 40 cm distal to the angle of Treitz, and terminus-terminus anastomosis was performed. The abdominal muscular and skin layers were closed in one layer using a continuous suturing technique.

Sleeve gastrectomy (SG) (n = 6) was performed by a laparotomy of 5 cm in the upper third of the abdomen, starting sectioning at the gastrosplenic ligament and exposing the stomach too, but this time, curved forceps were applied from the angle of Hiss to antrum, performing a cylindrical stomach of approximately 0.5 cm in diameter. The stomach sectioned resected the most fundus, stomach-corpus at greater curvature and antrum, preserving the pylorus. SG reduced the initial stomach volume by approximately 20 %. Reproducing the actual selective technique used in humans. Abdominal layers were closed as above.

In the RYGB group of rats (n = 6), a laparotomy of 3 cm was made in the midline of the abdomen, and a gastric pouch with a volume of approximately 30 % of the normal gastric volume was created. The remnant gastric fundus was anastomosed to the jejunum 14 cm distal from the ligament of Treitz. Abdominal layers were closed as above.

In the IR50 group of rats (n = 6), a small laparotomy of approximately 2–3 cm was performed at the abdominal midline. Once the small bowel was exposed, the distance between the Treitz angle and the ileum-caecal valve, was measured. Fifty percent of the intestine was resected, preserving 25 % of the small intestine distal to the Treitz angle and 25 % proximal to the ileocaecal valve. Finally, the abdominal layers were closed as described above.

### 2.3. Weight measurement

Weight gain was measured every 24 h for each animal from the FC, Sham, SG, RYGB and IR50 groups over twenty days after surgery and expressed as medium daily weight gain in grams.

### 2.4. Oral glucose tolerance test and insulin measurement

Twenty-seven and hundred sixty days after surgery, an oral glucose tolerance test (OGTT) was performed in FC, Sham, SG, RYGB and IR50 12-hour fasting rats. A 2 g/kg 20 % w/v D-glucose solution was administered using gavage. Glycaemia was measured by glucometer Glucocard G-Metre 1810 (Menarini Diagnostics, Italy) from blood samples obtained from rat tail veins 0, 30, 60, 90 and 120 min after glucose solution administration. The results obtained were expressed as glucose mg/plasma dl.

Plasma insulin measurement was performed four and twenty-three weeks after surgery in blood samples obtained from rat tail veins every 15 min for 60 min after glucose solution administration. We used an ELISA kit (ALPCO Diagnostics, Salem, NH) according to the manufacturer's instructions. The area under the curve (AUC) was calculated by the trapezoidal rule for plasma glucose and plasma insulin data in the study.

### 2.5. Somatostatin measurement

Twenty-three weeks after surgery, a 4 ml/kg, 13.9 KJ/ml mixed meal was administered to the 12-hour fasting rats from each group by oral gavage. Blood samples obtained from the FC, Sham, SG, RYGB and IR50 rat tail veins were added to EDTA, centrifuged at 4.000 G for 15 min at 4 °C, every 15 min for 120 min. Plasma was removed and stored at −80 °C. Total-SST, SST-14 and SST-28 plasma fractions were assessed by sandwich ELISA kits (MyBioSource Inc, San Diego CA, USA; BMA-Biomedicals, CH-4302, Augst, Switzerland) according to the manufacturer's instructions. SST values obtained for plasma SST were expressed as pg/ml. The total SST area under the curve (AUC) was calculated by the trapezoidal rule in the study.

### 2.6. Sacrifice, tissue processing and immunohistochemistry

The animals were sacrificed twenty-four weeks after surgery by isoflurane inhalation overdose. A portion of the brain containing hypothalamus, duodenum and pancreas were immediately removed and fixed in Bouin's solution overnight at 4 °C. The samples were dehydrated, embedded in paraffin and cut into serial 8 µm microtome sections.

In these rehydrated sections of a portion of hypothalamus containing periventricular nucleus, duodenum and pancreas, SST-producing cell populations were analysed by immunostaining using rabbit anti-somatostatin IgG antibody (Abcam Cambridge, CB4 OFL, UK) and mouse anti-insulin IgG antibody (Sigma Aldrich, St Louis MO, USA). The fluorescent secondary antibodies were Alexa 488 and 546 (Molecular Probes Inc. Eugene, OR, USA). DAPI was used to counterstain nuclei.

Beta-cell mass was evaluated by multiplying the positive islet area/total pancreatic area ratio by the total pancreatic weight (insulin-positive islet area). The results were expressed as milligrams (mg).

The SST-positive cell number was measured in five slices of the hypothalamus or duodenum and 25 pancreatic islets per condition and expressed as the number of SST-positive cells/mm$^2$ of tissue or islets in the case of the pancreas.

### 2.7. Statistical analysis

Data are presented as the mean ± SEM. For secretion patterns, AUC and histological data analysis, one-way ANOVA followed by Tukey's/Bonferroni post hoc test was conducted using SPSS V24.0 software. The correlation between SST-28 plasma values and pancreatic delta-cell expression was determined by Pearson´s coefficient value. Statistical significance was accepted at $P < 0.05$ (*, #) or $P < 0.01$ (**, ##).

## 3. Results

### 3.1. Weight gain

We measured the weight gain in the FC, Sham, SG, RYGB and IR50 groups twenty days after surgery, as Fig. 1 indicates. There were no differences between the control groups from the first day to the twentieth day. However, significant differences were observed between the control groups and the RYGB group beginning on the seventeenth day ($P < 0.05$) or between the SG and IR50 with respect to the control groups since the nineteenth day ($P < 0.05$).

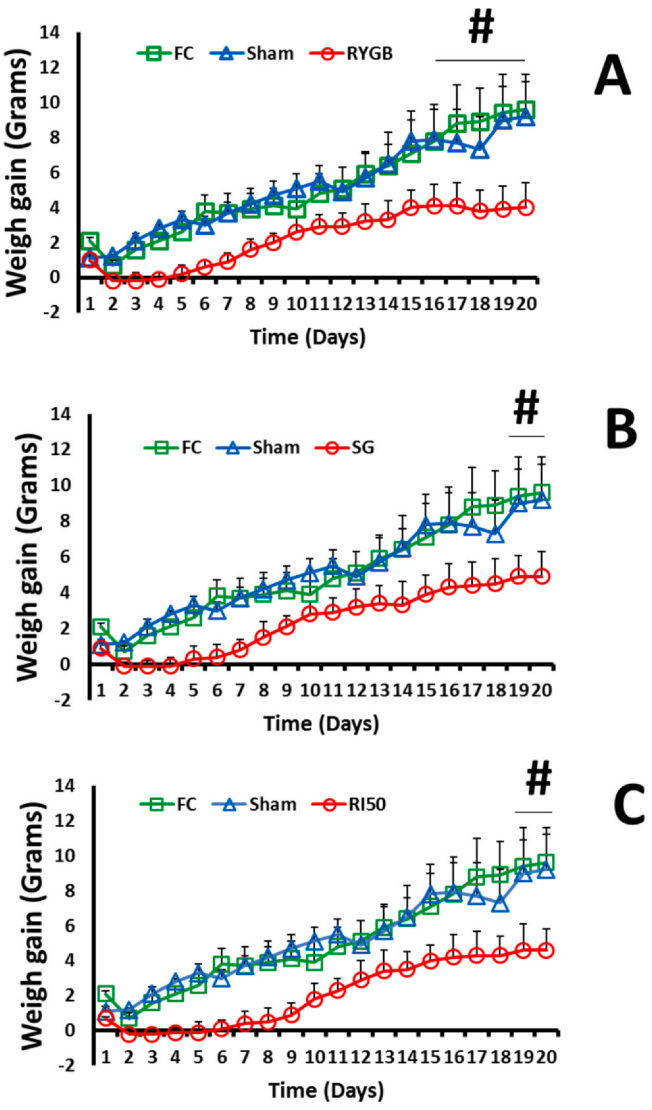


**Fig. 1.** Fig. 1A: Weight gain in n = 6 Fasting control rats (FC, green line with squares); n = 6 Sham-operated rats (blue line with triangles); n = 6 RYGB-operated rats (red line with circles). Fig. 1B: The FC and Sham groups are represented in Fig. 1A; n = 6 SG-operated mice are represented by red lines with circles. Fig. 1C: The FC and Sham groups are represented in Fig. 1A; n = 6 IR50-operated rat weights are represented by red lines with circles. Weight gain was expressed as grams on the Y axis, and time was expressed as days on the X axis. Values are represented as the mean ± SEM. Significant differences at $P < 0.05$ are marked as (#).

### 3.2. Oral glucose tolerance test (OGTT)

At the fourth and twenty-third weeks after surgery, an oral glucose tolerance test (OGTT) was performed, and the area under the curve (AUC) was calculated in all groups. As shown in Fig. 2A, 2C, 2E and 2G, no differences appeared between glucose tolerance patterns and AUCs between the five groups of rats four weeks after surgery. However, a significantly higher plasma glucose level appeared after glucose challenge in the SG group than in the control group twenty-three weeks after surgery (Fig. 2B). The AUC was calculated in SG rats ($P < 0.05$) (Fig. 2H). High plasma glucose levels were observed at 30 and 60 min after glucose administration in RYGB rats versus controls (Fig. 2D), with increased AUC compared with controls twenty-three weeks after surgery ($P < 0.05$) (Fig. 2H). Similar long-term glucose

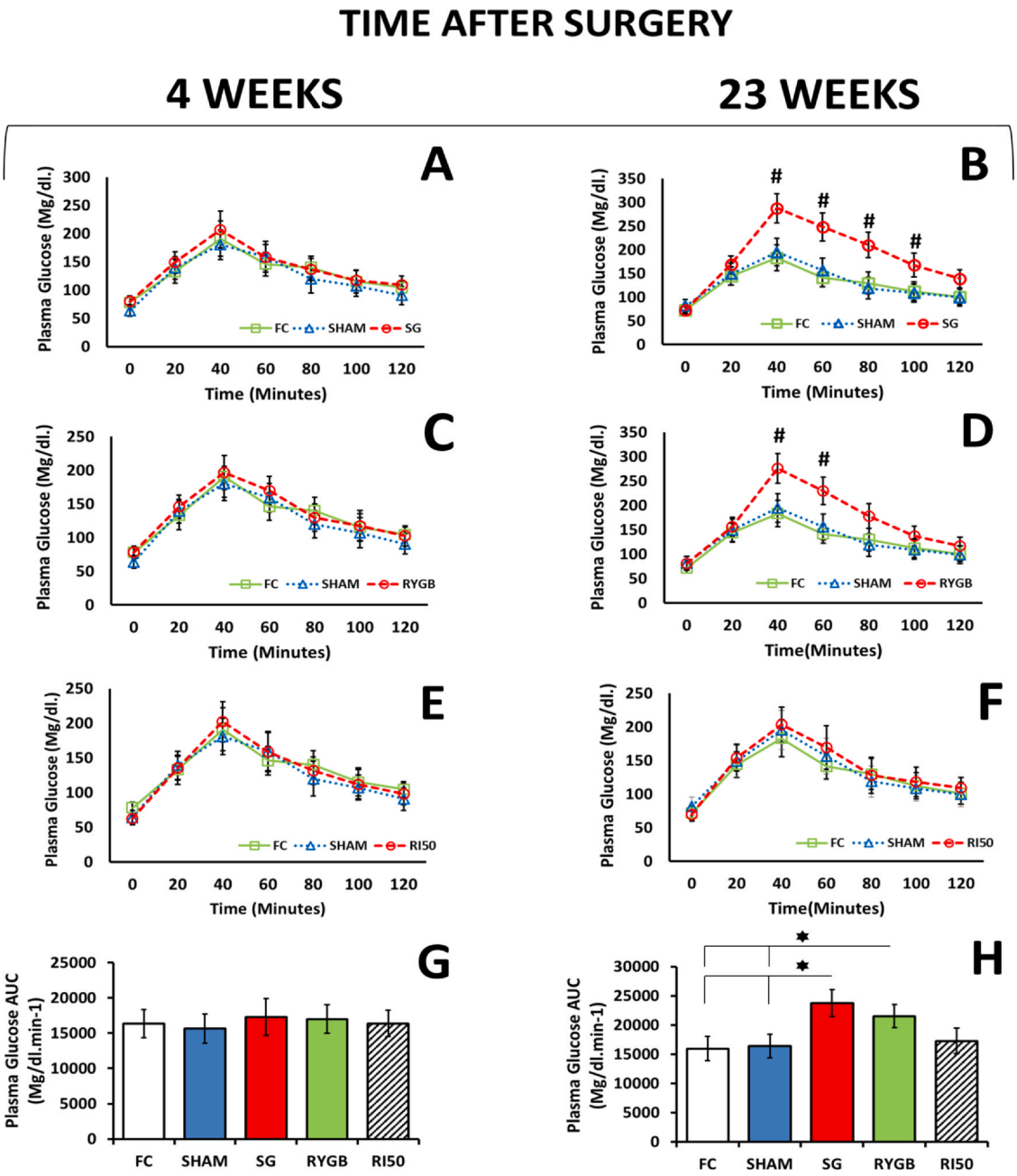


**Fig. 2.** Fig. 2A: Oral glucose tolerance test (OGTT) at the fourth week in n = 6 fasting control rats (FC, green line with squares); n = 6 sham-operated rats (blue line with triangles); and n = 6 SG-operated rats (red line with circles). Fig. 2C: The FC and Sham groups are represented in Fig. 2A; the n = 6 RYGB-operated plasma glucose pattern is represented by a red line with circles. Fig. 2E: The FC and Sham groups are represented in Fig. 2A; n = 6 IR50-operated plasma glucose patterns are represented by red lines with circles. Fig. 2G: Glucose area under the corresponding curve (AUC) values 4 weeks after surgery are presented as mg/dl min-1 on the Y axis for each group on the X axis. Fig. 2B: Oral glucose tolerance test (OGTT) at twenty-third week in n = 6 fasting control rats (FC, green line with squares); n = 6 sham-operated rats (blue line with triangles); and n = 6 SG-operated rats (red line with circles). Fig. 2D: The FC and Sham groups are represented in Fig. 2B; the n = 6 RYGB-operated plasma glucose pattern is represented by a red line with circles. Fig. 2F: The FC and Sham groups are represented in Fig. 2B; n = 6 IR50-operated plasma glucose patterns are represented by red lines with circles. Fig. 2H: Plasma glucose area under the corresponding curve (AUC) values 23 weeks after surgery are presented as mg/dl min-1 on the Y axis for each group on the X axis. All values are expressed as the mean ± SEM in each group. Significant differences at $P < 0.05$ are marked as (#) or (*).

tolerance patterns were found in the IR50 group with respect to the controls (Fig. 2F and 2H).

### 3.3. Insulin Assay

At the fourth and twenty-third weeks after surgery, plasma insulin measurements were performed after the oral glucose tolerance test (OGTT), and the insulin area under the curve (AUC) was calculated in the FC, Sham, SG, RYGB and IR50 groups. As Fig. 3C and 3E shows, an elevated insulin response appeared in RYGB and IR50 animals four weeks after surgery. However, the plasma insulin response pattern decreased from fifteen minutes to the end of the challenge in SG, RYGB and IR50 animals twenty-three weeks after surgery ($P < 0.05$) (Fig. 3B, 3D and 3F).

The plasma insulin AUC observed four weeks after surgery was significantly higher in the SG, RYGB and IR50 groups than in the control groups ($P < 0.05$) (Fig. 3G). Alternatively, at the end of the study, twenty-three weeks after surgery, low plasma insulin AUC values were detected in SG, RYGB and IR50 with respect to controls ($P < 0.05$), as Fig. 3H shows.

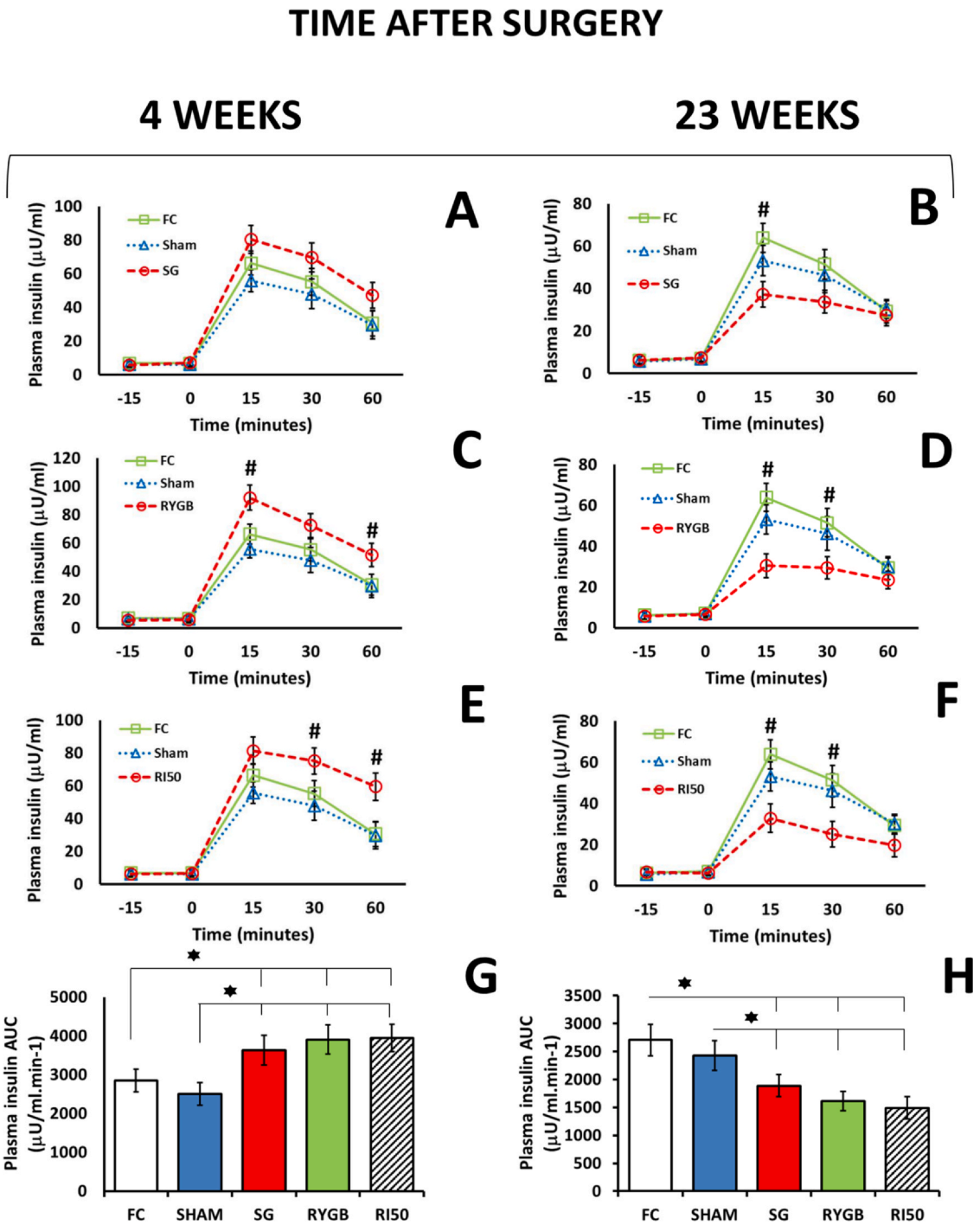


**Fig. 3. :** Insulin measurement after glucose challenge at the fourth week in n = 6 Fasting control rats (green line with squares); n = 6 Sham-operated rats (blue line with triangles); and n = 6 SG-operated rats (red line with circles). Fig. 3C: The FC and Sham groups are represented in Fig. 3A; n = 6 RYGB-operated insulin release patterns are represented by red lines with circles. Fig. 3E: The FC and Sham groups are represented in Fig. 3A; n = 6 IR50-operated insulin release patterns are represented by red lines with circles. Fig. 3G: Insulin area under the corresponding curve (AUC) values 4 weeks after surgery are presented as µU/ml min-1 on the Y axis for each group on the X axis. Fig. 3B: Insulin measurement after glucose challenge at the twenty-third week in n = 6 Fasting control rats (green line with squares); n = 6 Sham-operated rats (blue line with triangles); and n = 6 SG-operated rats (red line with circles). Fig. 3D: The FC and Sham groups are represented in Fig. 3B, and the n = 6 RYGB-operated insulin release pattern is represented by a red line with circles. Fig. 3F: The FC and Sham groups are represented in Fig. 3B, and n = 6 IR50-operated insulin release patterns are represented by red lines with circles. Fig. 3H: Insulin area under the corresponding curve (AUC) values 23 weeks after surgery are presented as µU/ml min-1 on the Y axis for each group on the X axis. All values are expressed as the mean ± SEM in each group. Significant differences at P < 0.05 are marked as (#) or (*).

### *3.4. Somatostatin analysis*

We measured the circulating plasma fraction of total SST, SST-28 and SST-14 after oral mixed-meal administration in the five study groups at twenty-three weeks after surgery. An enhanced total SST secretion pattern appeared after mixed-meal administration in SG rats but not in RYGB or IR50 rats with respect to the control groups (P < 0.05) (Fig. 4B and 4C). This situation was reflected in the AUC values with a significantly different and increased red bar with respect to controls (P < 0.05) (Fig. 4D).

Additionally, we assayed SST-28 and SST-14 plasma fractions. A significantly lower SST-14 plasma fraction was detected in SG rats

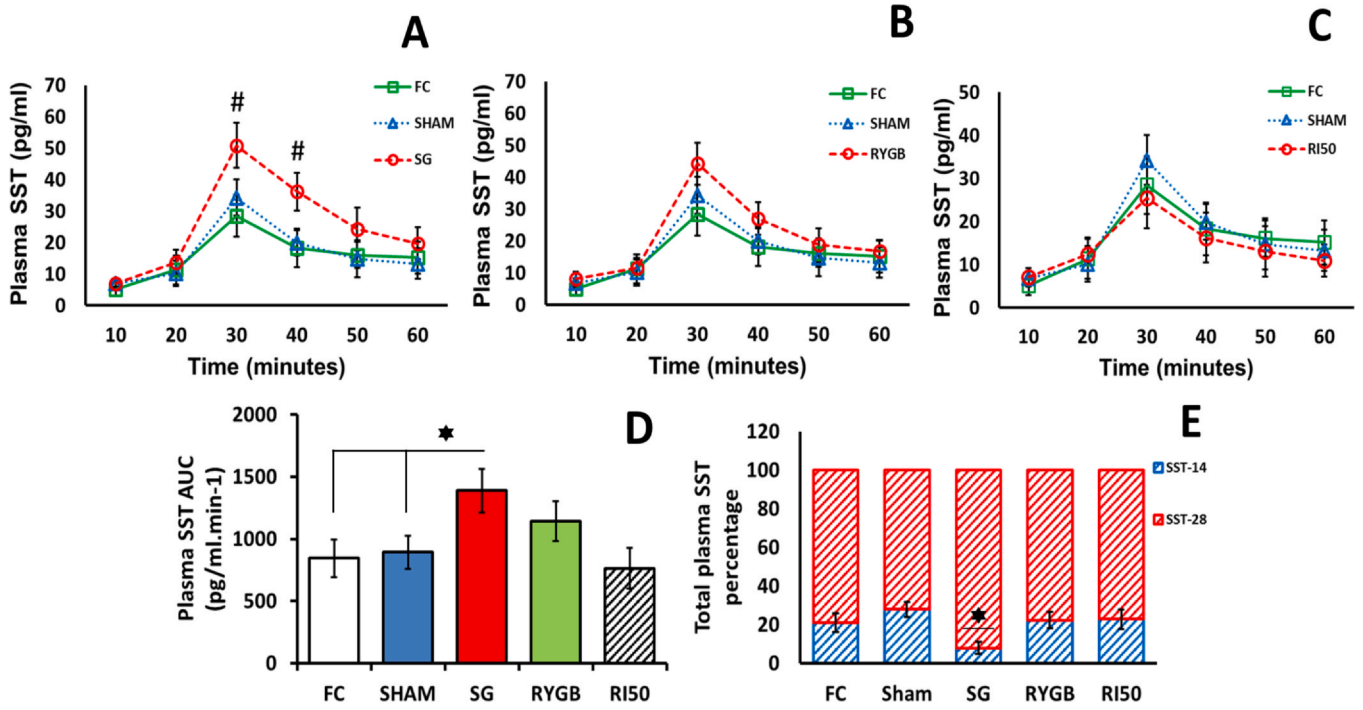


**Fig. 4. :** Plasma somatostatin level analysis twenty-three weeks after surgery. Fig. 4A: Plasma total-SST secretion pattern after mixed meal administration. n = 6 Fasting control rats (green line with squares), n = 6 Sham-operated rats (blue line with triangles) and n = 6 SG-operated rats (red line with circles). Fig. 4B: The FC and Sham groups are represented in Fig. 4A; n = 6 RYGB-operated plasma total-somatostatin patterns are represented by the red line with circles. Fig. 4C: The FC and Sham groups are represented in Fig. 4A; n = 6 IR50-operated plasma total-somatostatin pattern is represented by the red line with circles. Fig. 4D: Plasma total-somatostatin area under the corresponding curve (AUC) values 23 weeks after surgery are presented as pg/ml min-1 on the Y axis for each group on the X axis. Fig. 4E: SST-14 and SST-28 fractions of plasma total SST in every group after mixed meal administration four and twenty-three weeks after every group on the X axis; the Y axis represents the average percentage of plasma SST-14 (blue striped bar) and SST-28 (red striped bar). Significant differences at P < 0.05 are marked as (#) or (*).

but not in RYGB or IR50 groups or in controls groups (P < 0.05) (Fig. 4E).

### 3.5. SST tissue expression

Twenty-four weeks after surgery, SST-producing cell expression was analysed by immunostaining in three tissue samples (hypothalamus, duodenum and pancreatic islet) from each group. We expressed the values as the number of SST-positive cells/mm$^2$ of each tissue area.

As Fig. 5A shows, no differences were found between hypothalamic SST-producing cell expression in the control and surgical groups. However, Fig. 5B displays a high number of SST-positive cells in the duodenum from SG and RYGB-operated rats versus IR50-operated rats or controls (P < 0.01; P < 0.05). Alternatively, a low SST-producing cell population was detected in pancreatic islets from the SG and RYGB groups but not in the IR50 and control groups (P < 0.01; P < 0.05), as shown in Fig. 5C.

AUCs of the SST-28 plasma fraction at twenty-three weeks post-surgery were correlated with SST-producing cell expression in the duodenum (number of SST-positive cells/mm$^2$ of duodenum). We observed a strong direct correlation between the two parameters, as shown in Fig. 5D (R2 =0.868; P < 0.05). Finally, the AUCs of SST-28 plasma fraction weeks were correlated with SST-producing cell expression in the pancreas (delta-cell population). We showed an inverse correlation between the two parameters (R2 =0.571; P < 0.05) (Fig. 5E).

## 4. Discussion

The role of SST in T2DM improvement after bariatric surgery has been understudied, likely due to the multiple places where the isoforms can be released. In this way, we analysed the three most important SST-secreting tissues after surgery in each group.

As we observed in Fig. 5A to 5C, a significant increase in SST-positive cells appeared in duodenum samples after SG and RYGB but not after IR50. This finding leads us to think about a compensatory response after the stomach ablation of SST-producing cells, which correlates with the duodenal SST expression observed, which is proportional to the amount of gastric tissue removed; thus, the expression is greater in the SG versus IR50 group, where there is no gastric resection. These data are supported by previous work confirming this effect after SG (Pérez-Arana et al., 2022a,2022b). Also based on our supplementary data (accessory Fig. 2), glucagon secretion does not seem to be affected in the medium or long term by changing somatostatin levels. In this way, there would be a synergistic effect between beta-cell population exhaustion due somatostatin brake loss, with a high initial insulin response and the inhibitory effect of sustained glucagon secretion in the final stage of the experiment.

In addition, high plasma levels of total SST and SST-28 were found in rats after SG but not after RYGB, IR50 or in controls (Fig. 4). Interestingly, the RYGB total-SST and SST-28 plasma fractions were lower than those found in SG rats. These data lead us to think about a proportional response to each type of surgery. This progressive and proportional response according to stomach surgical damage is consistent with the proposal by many authors who claim that SST-28 is mainly secreted in the duodenum at the total postprandial SST plasma level (D´Alessio and Ensinck, 1990; Gutniak et al., 1987).

Alternatively, a decreased beta-cell mass was found twenty-four weeks after surgery in SG, RYGB and IR50 animals with respect to the fasting control and Sham groups (accessory Fig. 1). These data could explain the significant low insulin AUC values observed at twenty-three weeks in SG, RYGB and IR50 animals (Fig. 3B, 3D, 3F and 3H). This reduced insulin response could be the result of a beta-cell mass exhaustion

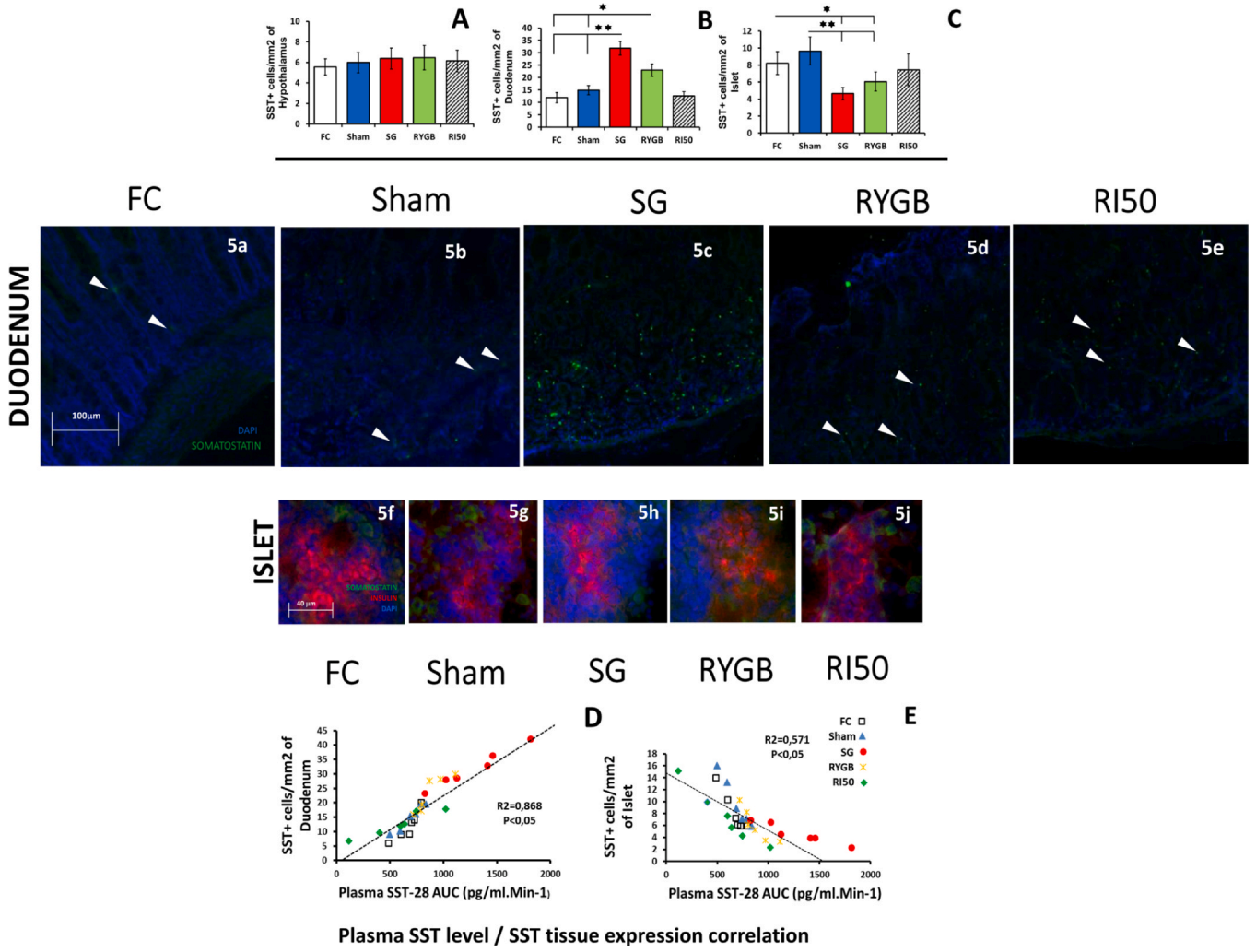


**Fig. 5. :** Somatostatin tissue expression analysis. Fig. 5A, 5B and 5C: Hypothalamic, duodenal and islet somatostatin expression twenty-four weeks after surgery. On the X axis: n = 6 FC rats (white bar); n = 6 Sham rats (blue bar); n = 6 SG-operated rats (red bar); n = 6 RYGB-operated rats (green bar); and n = 6 IR50-operated rats (black striped bar). On the Y axis, the number of SST-positive cells per $mm^2$ is expressed as the mean ± SEM. Fig. 5D: SST expression in the duodenum and plasma SST-28 level correlation in each group; n = 6 FC rats (withe squares), n = 6 Sham rats (blue triangles), n = 6 SG rats (red circles), n = 6 RYGB rats (yellow crosses) and n = 6 IR50 rats (green diamonds). Fig. 5E: SST expression in pancreatic islets and plasma SST-28 level correlation in each group; n = 6 FC rats (withe squares), n = 6 Sham rats (blue triangles), n = 6 SG rats (red circles), n = 6 RYGB rats (yellow crosses) and n = 6 IR50 rats (green diamonds). Significant differences at $P < 0.05$ are marked as (*). Images 5a to 5e represent (20x) SST expression in the duodenum from FC, Sham, SG, RYGB and IR50 rats twenty-four weeks after surgery. SST expression was immunostained in green (Alexa 488), and DAPI was used to counterstain nuclei. Images 5 f to 5j represent (20x) SST expression in pancreatic islets from FC, Sham, SG, RYGB and IR50 rats twenty-four weeks after surgery. SST expression was immunostained green (Alexa 488), insulin was immunostained red (Alexa 546), and DAPI was used to counterstain nuclei.

stage due to a previous period of hypersecretion. This situation has been described by previous works (Bancalero-de los Reyes et al., 2021; Pérez-Arana et al., 2022a,2022b).

Surprisingly, a strong decrease in pancreatic delta cells was observed in animals after SG and to a lesser extent that was not significant after RYGB and not in IR50 animals as Fig. 5C shows. This finding made us wonder about the relationship between the two phenomena. The high SST-28 plasma level and the depletion of the delta-cell population were observed after SG but not RYGB or IR50. To answer this question, we analysed the correlation between SST-28 plasma levels and delta-cell expression in the pancreas (accessory Fig. 2), and a low inversely proportional relationship appears between them. However, we cannot guarantee linearity. Regardless, these data are not reliable given the low number of animals studied (n = 6) in each group. Thus, slight plasma SST-28 variations might imply great pancreatic delta-cell expression variations beyond a certain threshold. This is an interesting issue and could be the subject of future studies.

Nevertheless, taking the entire dataset, these results could explain SG diabetes improvement by intrapancreatic SST-14 decrease and therefore loss of the SST-14 brake on the secretory capacity of beta-cells (Perez et al., 2022a). However, it does not appear to be valid to explain the diabetes improvement after RYGB as this technique cannot modify the delta-cell population, so this finding is likely due to the small portion of SST-28. The producing tissue is removed in RYGB, which is insufficient to trigger a strong compensatory response in the duodenum. Image 1 illustrates the physiopathological mechanism proposed to explain the hyperinsulinaemic response after each surgery.

Moreover, RYGB is a more complex intervention than SG involving not only stomach affectation but also anatomical rearrangements of the small intestine. In this way, the intervention of other gastrointestinal hormones, such as PYY and/or GLP-1, in the changes of the endocrine pancreas after surgery seems to make sense. As indirect probes, plasma levels of PYY and GLP-1 were tested in the three groups (Camacho-Ramírez et al., 2020a, 2020b). Significant

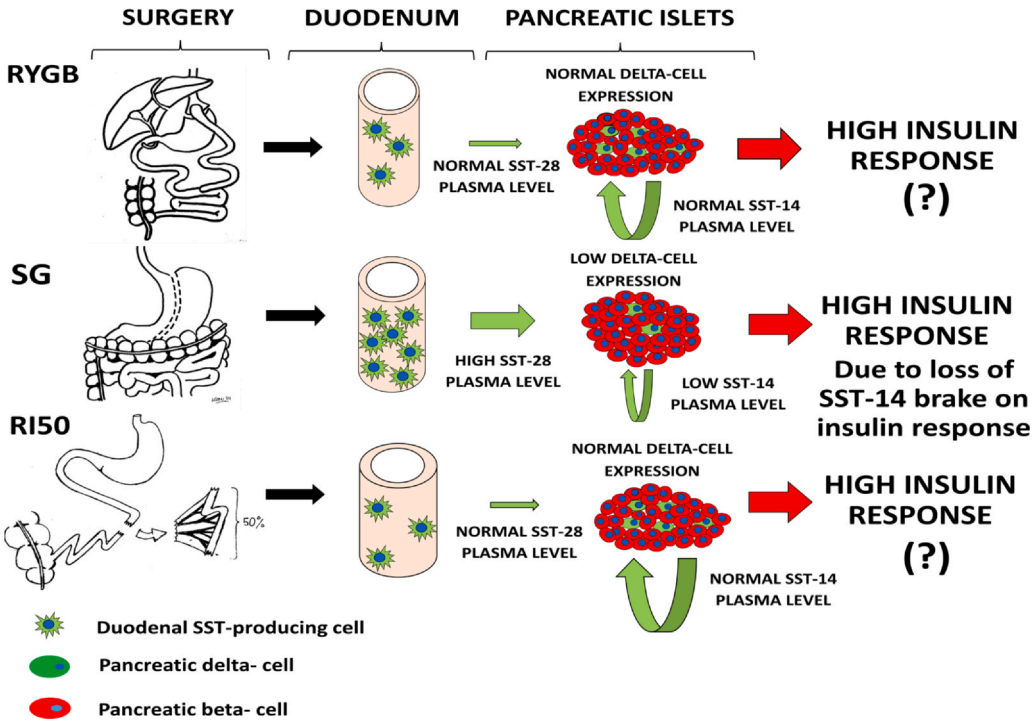


**Image 1.** Representative diagram of the effect of different bariatric/metabolic surgeries on SST expression in the duodenum and pancreas. There are at least two mechanisms. One is initiated by the ablation of SST-28-producing cells in the stomach and the consequent compensatory SST-28 hyperexpression in the duodenum. SST-28-producing cell resection was major after SG, partial after RYGB and unaffected after IR50 and controls. Another possibility could be mediated by different processes that do not affect the delta-cell population, but this would explain the effects of RYGB and IR50 on glucose metabolism. In any case, further understanding of both mechanisms is needed.

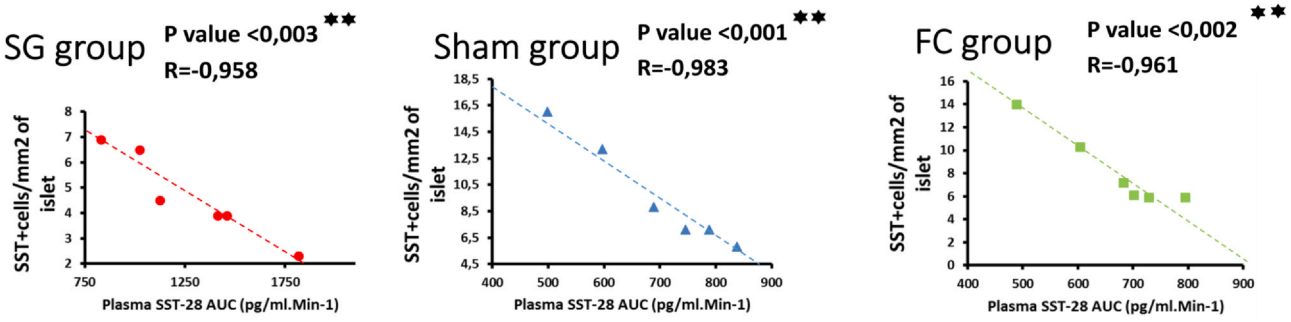


**Accessory Figure 1.**

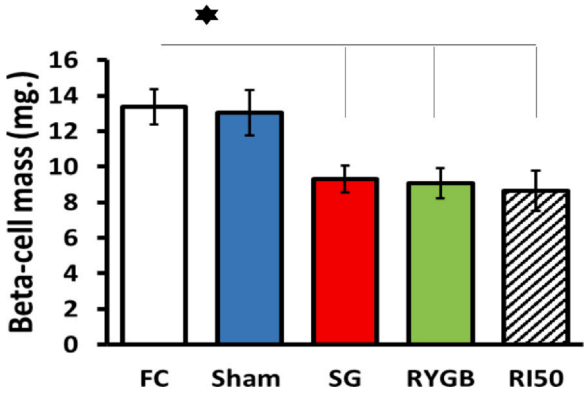


**Accessory Figure 2.**

differences appeared between these surgical techniques (RYGB and SG), confirming considerably different mechanisms. Even with these different biological mechanisms, the last consequence reaches a common pancreatic point of aggression after a long-lasting period after surgery. The common final consequences are beta-cell population exhaustion and long-term insulin response depletion. These are the basis of bariatric surgery failure after a long period of metabolic improvement in patients.

In conclusion, we can say that in our model, the compensatory response to the loss of somatostatin-producing gastric tissue is the pathophysiological mechanism that leads to a strong insulin response after SG but not in the other surgeries. On the other hand, the same long-term mechanism triggers the beta-cell population exhaustion and insulin response depletion.

Today, SG is a widely performed surgery. Therefore, as SST-28 plasma level seems to be involved in these mechanisms, the restriction of the resected gastric tissue or the use of SST-28 agonists after surgery could improve long –term outcomes for SG surgery. Limiting the duodenal compensatory response to gastric SST-producing cells ablation and preventing the long-term beta-cell population exhaustion. However, maintaining the balance without losing the effect of surgery on glucose metabolism is difficult and needs further study, both in animals and in patients.

## CRediT authorship contribution statement

A Camacho, G Pérez-Arana and JA Prada designed the project. D Almorza and J Bancalero analysed the procedures for statistical analysis. A Diaz, J Bancalero, A Camacho, A Ribelles, and I Mateo performed the surgical techniques, followed the animal survival period and performed the functional tests. G Pérez-Arana directed the histological techniques. All authors participated in preparing the manuscript.

## Declaration of Competing Interest

The authors declare that they have no known competing financial interests or personal relationships that could have appeared to influence the work reported in this paper.

## Acknowledgements and Grant support

We fully appreciate the technical assistance of Ms. María Reyes Ruz Velázquez, medical degree student at the Anatomy and Embryology Department of Cádiz. The authors would like to thank the Vicechancelor of Research Policies and INIBICA Institute (University of Cádiz). The authors thanks to Tugiana-Peal of Becerro Association for the grant support.

## References

Alsumali, A., Eguale, T., Bairdain, S., Samnaliev, M., 2018. Cost-effectiveness analysis of bariatric surgery for morbid obesity. Obes. Surg. 28, 2203–2214. https://doi.org/10.1007/s11695-017-3100-0

Bancalero-de los Reyes, J., Camacho-Ramírez, A., Fernández-Vivero, J., Ribelles-García, A., Macías-Rodríguez, M., Almorza-Gomar, D., Carrasco-Molinillo, C., Mayo-Ossorio, M.A., Prada-Oliveira, J.A., Perez-Arana, G., 2021. Glucagon-producing cell expansion in Wistar rats. Changes to islet architecture after sleeve gastrectomy. Obes. Surg. 31, 2241–2249. https://doi.org/10.1007/s11695-021-05264-6

Benaiges, D., Más-Lorenzo, A., Goday, A., Ramon, J.M., Chillarón, J.J., Pedro-Botet, J., Flores-Le Roux, J.A., 2015. Laparoscopic sleeve gastrectomy: more than a restrictive bariatric surgery procedure? World J. Gastroenterol. 21 (41), 11804–11814. https://doi.org/10.3748/wjg.v21.i41.11804

Benso, A., Gottero, C., Prodam, F., Gauna, C., Destefanis, S., Filtri, L., van der Lely, A.J., Deghenghi, R., Ghigo, E., Broglio, F., 2003. Effects of cortistatin-14 and somatostatin-14 on the endocrine response to hexarelin in humans. J. Endocrinol. Invest. 26 (7), 599–603. https://doi.org/10.1007/BF03347014

Camacho-Ramírez, A., Mayo-Ossorio, M.A., Pacheco-García, J.M., Almorza-Gomar, D., Ribelles-García, A., Belmonte-Núñez, A., Prada-Oliveira, J.A., Pérez-Arana, M., 2020a. Pancreas is a preeminent source of ghrelin after sleeve gastrectomy in Wistar rats. Histol. Histopathol. 35 (8), 801–809. https://doi.org/10.14670/HH-18-200

Camacho-Ramírez, A., Prada-Oliveira, J.A., Ribelles-García, A., Almorza-Gomar, D., Pérez-Arana, G.M., 2020b. The leading role of peptide tyrosine tyrosine in glycemic control after Roux-en-Y gastric bypass in rats. Obes. Surg. 30 (2), 697–706. https://doi.org/10.1007/s11695-019-04239-y

D'Alessio, D.A., Ensinck, J.W., 1990. Fasting and postprandial concentrations of somatostatin-28 and somatostatin-14 in type II diabetes in men. Diabetes 39 (10), 1198–1202. https://doi.org/10.2337/diab.39.10.1198

Francis, B.H., Baskin, D.G., Saunders, D.R., Ensinck, J.W., 1990. Distribution of somatostatin-14 and somatostatin-28 gastrointestinal-pancreatic cells of rats and humans. Gastroenterology 99 (5), 1283–1291. https://doi.org/10.1016/0016-5085(90)91151-u

Guida, C., McCulloch, L.J., Godazgar, M., Stephen, S.D., Baker, C., Basco, D., Dong, J., Chen, D., Clark, A., Ramracheya, R.D., 2018. Sitagliptin and Roux-en-Y gastric bypass modulate insulin secretion via regulation of intra-islet PYY. Diabetes Obes. Metab. 20 (3), 571–581. https://doi.org/10.1111/dom.13113

Guida, C., Stephen, S.D., Watson, M., Dempster, N., Larraufie, P., Marjot, T., Cargill, T., Rickers, L., Pavlides, M., Tomlinson, J., Cobbold, J., Zhao, C.M., Chen, D., Gribble, F., Reimann, F., Gillies, R., Sgromo, B., Rorsman, P., Ryan, J.D., Ramracheya, R.D., 2019. PYY plays a key role in the resolution of diabetes following bariatric surgery in humans. EBioMedicine 40, 67–76. https://doi.org/10.1016/j.ebiom.2018.12.040

Gutniak, M., Grill, V., Wiechel, K.L., Efendić, S., 1987. Basal and meal-induced somatostatin-like immunoreactivity in healthy subjects and in IDDM and totally pancreatectomized patients. Effects of acute blood glucose normalization. Diabetes 36 (7), 802–807. https://doi.org/10.2337/diab.36.7.802

McTigue, K.M., Wellman, R., Nauman, E., Anau, J., Coley, R.Y., Odor, A., Tice, J., Coleman, K.J., Courcoulas, A., Pardee, R.E., Toh, S., Janning, C.D., Williams, N., Cook, A., Sturtevant, J.L., Horgan, C., Arterburn, D., 2020. Bariatric study collaborative comparing the 5-year diabetes outcomes of sleeve gastrectomy and gastric bypass: the national patient-centered clinical research network (PCORNet) Bariatric Study. JAMA Surg. 155 (5), e200087. https://doi.org/10.1001/jamasurg.2020.0087

Mokadem, M., Zechner, J.F., Margolskee, R.F., Drucker, D.J., Aguirre, V., 2013. Effects of Roux-en-Y gastric bypass on energy and glucose homeostasis are preserved in two mouse models of functional glucagon-like peptide-1 deficiency. Mol. Metab. 3, 191–201.

Mun, E.C., Blackburn, G.L., Matthews, J.B., 2001. Current status of medical and surgical therapy for obesity. Gastroenterology 120 (3), 669–681. https://doi.org/10.1053/gast.2001.22430

Nauck, M., 2016. Incretin therapies: highlighting common features and differences in the modes of action of glucagon-like peptide-1 receptor agonists and dipeptidyl peptidase-4 inhibitors. Diabetes Obes. Metab. 18 (3), 203–216. https://doi.org/10.1111/dom.12591

Pérez-Arana, G.M., Díaz-Gómez, A., Bancalero, J., Camacho-Ramírez, A., Ribelles-García, A., Almorza-Gomar, D., Gracia-Romero, M., Mateo-Gavira, I., Prada-Oliveira, A. 2022b. Somatostatin is key to explaining the long-term effect of anatomical rearrangements after sleeve gastrectomy on glucose metabolism. Surg Obes Relat Dis. In press.

Pérez-Arana, G.M., Díaz-Gómez, A., Bancalero, J., Camacho-Ramírez, A., Fernández-Vivero, J., Ribelles-García, A., Almorza-Gomar, D., Carrasco-Molinillo, C., Mateo-Gavira, I., Prada-Oliveira, A., 2022a. The long-term failure of RYGB surgery in improving T2DM is related to hyperinsulinism. Ann. Anat. 240, 151855. https://doi.org/10.1016/j.aanat.2021.151855

Santiago-Fernández, C., García-Serrano, S., Tome, M., Valdes, S., Ocaña-Wilhelmi, L., Rodríguez-Cañete, A., Tinahones, F.J., García-Fuentes, E., Garrido-Sánchez, L., 2017. Ghrelin levels could be involved in the improvement of insulin resistance after bariatric surgery. Endocrinol. Diabetes Nutr. 64, 355–362. https://doi.org/10.1016/j.endinu.2017.05.002

Schauer, P.R., Deepak, L.B., Kirwan, J.P., Wolski, K., Aminian, A., Brethauer, S.A., Navaneethan, S.D., Singh, R.P., Pothier, C.E., Nissen, S.E., Kashyap, S.R., 2017. STAMPEDE Investigators. Bariatric surgery versus intensive medical therapy for diabetes - 5-Year Outcomes. N. Engl. J. Med. 376 (7), 641–651. https://doi.org/10.1056/NEJMoa1600869

Shah, M., Laurenti, M.C., Man, C.D., Ma, J., Cobelli, C., Rizza, R.A., Vella, A., 2019. Contribution of endogenous glucagon-like peptide-1 to changes in glucose metabolism and islet function in people with type 2 diabetes four weeks after Roux-en-Y gastric bypass (RYGB). Metabolism 93, 10–17. https://doi.org/10.1016/j.metabol.2018.12.005

Xu, S.F.S., Andersen, D.B., Izarzugaza, J.M.G., Kuhre, R.E., Holst, J.J., 2020. In the rat pancreas, somatostatin tonically inhibits glucagon secretion and is required for glucose-induced inhibition of glucagon secretion. Acta Physiol. (Oxf.) 229 (3), e13464. https://doi.org/10.1111/apha.13464